The Influence of a Resolved Gulf Stream on the Decadal Variability of Southeast US Rainfall

Wei Zhang[1,2]*; Ben Kirtman[3]; Leo Siqueira[3]; Baoqiang Xiang[2,4]; Johnna Infanti[5]; Natalie Perlin[3]

1 Program in Atmospheric and Oceanic Sciences, Princeton University, Princeton, NJ, USA.
2 NOAA/Geophysical Fluid Dynamics Laboratory, Princeton, NJ, USA.
3 Rosenstiel School of Marine and Atmospheric Science, University of Miami, Miami, USA.
4 Cooperative Programs for the Advancement of Earth System Science, University Corporation for Atmospheric Research, Boulder, CO, USA.
5 NOAA/NWS/NCEP/Climate Prediction Center, College Park, Innovim, LLC, Greenbelt, MD, USA.
***** Corresponding author: Wei Zhang (wz19@princeton.edu)

Key Points

- The Gulf Stream influences regional rainfall patterns in the Southeast US
- Eddying CCSM4 improves the representation of the North Atlantic Subtropical High variability and its connection to the Southeast US rainfall
- Eddy-parameterizing CCSM4 and CMIP5 models may overestimate the role of tropical sea surface temperature in decadal Southeast US rainfall

Abstract

Ocean variability is a dominant source of remote rainfall predictability, but in many cases the physical mechanisms driving this predictability are not fully understood. This study examines how ocean mesoscales (i.e., the Gulf Stream SST front) affect decadal southeast US (SEUS) rainfall, arguing that the local imprint of large-scale teleconnections is sensitive to resolved mesoscale features. Based on global coupled model experiments with eddying and eddy-parameterizing ocean, we find that a resolved Gulf Stream improves localized rainfall and remote circulation response in the SEUS. The resolved Gulf Stream influences the boundary layer, driving a barotropic circulation response, thus affecting decadal SEUS rainfall due to a westward extension of the North Atlantic Subtropical High. The eddy-parameterizing simulation fails to capture the sharp SST gradient associated with the Gulf Stream and overestimates the role of tropical SST in the SEUS rainfall due to its classical wintertime connection with the El Niño/Southern Oscillation.

Plain Language Summary

Current global climate models (GCMs) typically fail to fully resolve mesoscale ocean features (with length scales on the order of 10 km) such as western boundary currents, which potentially limit rainfall predictability over decadal timescales. Improvements in high-performance climate modeling enable us to incorporate high-resolution ocean models (0.1°) that capture these important mesoscale features with increased fidelity. Here we show that the inclusion of ocean mesoscales produces a more realistic Gulf Stream and improves both localized rainfall patterns and large-scale teleconnections. A resolved Gulf Stream drives a nearly barotropic circulation response and generally reproduces the observed variability of the North Atlantic Subtropical High that regulates Southeast US rainfall. The results further imply that high-resolution GCMs with increased ocean model resolution may be needed in future climate prediction systems.

1 Introduction

The ability to predict decadal rainfall variability over land remains one of the grand challenges in climate prediction. Regional prediction of rainfall has limited skill on timescales from seasons to decades (Hawkins & Sutton, 2011; Knutti & Sedláček, 2013; Kushnir et al., 2019; Pathak et al., 2019; Shepherd, 2014). For example, several recent studies have shown the underestimated signals in models, or the so-called "signal-to-noise paradox" (e.g., Scaife et al. 2014; Scaife & Smith, 2018; Siegert et al. 2016; Strommen & Palmer, 2019; Zhang et al., 2021; Zhang & Kirtman, 2019b) in decadal rainfall predictability (Smith et al., 2019, 2020), implying potentially serious issues in current modeling systems that fail to capture the observed decadal rainfall signals.

The ocean plays a crucial role in modulating low-frequency rainfall variability (see Battisti et al., 2019 for review of current understanding). Variations in sea surface temperature (SST) (e.g., El Niño/Southern Oscillation, ENSO) can result in substantial impacts on local air-sea feedbacks and teleconnection patterns affecting regional US precipitation variability (Grondona et al., 2000; Infanti & Kirtman, 2016; Mamalakis et al., 2018). However, extra-tropical mesoscale oceanic drivers of precipitation are not necessarily well represented in current GCMs (e.g., the fifth Coupled Model Intercomparison Project, CMIP5). In recent years, improvements in high-performance computing have enabled high-resolution GCMs with eddying (e.g., eddy-resolving and eddy-permitting) ocean models to include more mesoscale ocean processes (e.g., Delworth et al., 2012; Roberts et al., 2020; Wang et al., 2019; Zhang, 2020; Zhang et al., 2021). Studies with eddying GCMs show considerable benefits, for example, with better representation of ocean surface climatology (Kirtman et al., 2012; Siqueira & Kirtman, 2016), improvements in air-sea interactions (Bryan et al., 2010; Kirtman et al., 2017), and implications for remarkable impacts on precipitation changes especially over ocean regions (He et al., 2018).

Compared with their lower-resolution counterparts, eddying GCMs more accurately simulate fronts and the sharpness of SST gradients in the Gulf Stream (e.g., Siqueira & Kirtman, 2016) that are necessary to reproduce the observed distributions of the rainfall climatology (Bryan et al., 2010; Johnson et al., 2020; Minobe et al., 2008). Mesoscale air-sea interaction processes in the western boundary currents may influence the overlying atmospheric boundary layer and the upper troposphere and atmospheric circulation (Feliks et al., 2011; Siqueira et al., 2021; Small et al., 2008). However, whether and the degree to which the inclusion of ocean mesoscales affects remote regional precipitation over land – particularly decadal southeast US (SEUS) rainfall and teleconnections – remains unclear.

Low-frequency SEUS rainfall significantly responds to ocean surface conditions and large-scale patterns of SSTs such as ENSO, the Pacific Decadal Oscillation (PDO) (e.g., Fuentes-Franco et al., 2016; Li et al., 2012) and the Atlantic Multi-decadal Oscillation (AMO) (e.g., Burgman & Jang, 2015; Kwon et al., 2009). For instance, ENSO can play an essential role in modulating seasonal to interannual SEUS rainfall variability, especially during winter seasons (Hoerling et al., 1997; Infanti & Kirtman, 2019; Schmidt et al., 2001; Trenberth et al., 1998). The impacts of tropical cyclones (Chan & Misra, 2010; Knight & Davis,

2007; Nogueira & Keim, 2011) and surface soil moisture (Koster et al., 2004; Yoon & Leung, 2015) on SEUS rainfall have also been addressed in previous studies. Of particular interest here is the North Atlantic subtropical high (NASH). Li et al. (2011) and Li et al. (2012) have noted that the displacement of the NASH western ridge influences the SEUS rainfall in summer by changing the moisture transport and vertical motion. The westward extension of the NASH towards the continental US contributes to increased northward flow and low-level convergence, leading to upward motion and more precipitation over the SEUS.

Here we diagnose how mesoscale ocean features affect decadal-scale SEUS precipitation and teleconnections based on the hypothesis that SST variability associated with the Gulf Stream front affect the position of the NASH and hence rainfall over SEUS. Possible influences of SSTs and the NASH on the SEUS rainfall at decadal timescales is discussed based on a suite of global coupled model simulations with the Community Climate System Model Version 4.0 (CCSM4; Gent et al., 2011) using eddying and eddy-parameterizing ocean component models.

2 Data and Method

2.1 Data

Observed monthly precipitation data are obtained from the Global Precipitation Climatology Project (GPCP) version 2.3 combined precipitation dataset (1979-present; Adler et al., 2018) and the gauge-based Global Precipitation Climatology Center (GPCC) precipitation product (1901-2016; Schneider et al., 2017) from the National Center for Atmospheric Research (NCAR). The GPCP data has a 40-year record and lower resolution on global 2.5° grids, whereas the GPCC provides land-surface precipitation with 1°x1° spatial resolution and a long-time record. To represent the NASH variability, we use the geopotential heights at 850 hPa from the NOAA's twentieth-century reanalysis version-2c data (20CV2c; Compo et al., 2011).

We assessed thirty coupled models from CMIP5 that were used as supplementary analyses (Table S1). All CMIP5 models are considered as low-resolution GCMs with an eddy-parametrized ocean. To equally weight each model, we only consider the first realization of each model's historical simulation. The results based on CMIP5 models are analyzed and compared with observational estimates.

2.2 Model Experiments

To examine the influence of ocean mesoscales on climate simulations, we perform two different sets of experiments using CCSM4 with eddy-parameterizing (1° ocean; hereafter, LRC) and eddying (0.1°; hereafter, HRC) ocean components, respectively. CCSM4 is a fully coupled climate model consisting of component models for atmosphere, land, ocean, sea ice, and the coupling infrastructure. A general description of CCSM4 can be found in Gent et al. (2011).

In this study, the LRC experiment is a present-day control simulation (greenhouse gas concentrations for

1990) using 1° atmosphere/land coupled to the ocean and sea-ice models with the nominal 1° horizontal resolution. LRC is initialized with an ocean at rest and allows for 200 years of spin-up period and then a 300-year simulation is integrated for analysis (the same simulation as used in Zhang & Kirtman, 2019a). HRC experiments include three high-resolution simulations that are identical except for a small perturbation in the initial conditions. The initial condition for our first HRC simulation is taken from the end of the previously completed LRC experiment, and we ran the HRC model for 155-years and only analyzed the last 55-years. The two other HRC simulations are initialized, with small initial perturbations, at year 48 of the first, and run for 70-years. We drop the first 20-years of both of these simulations in our analysis. The details of CCSM4 HRC and LRC model experiments are discussed in Zhang et al. (2021).

To diagnose the potential impact of atmospheric resolutions, we perform an additional experiment (hereafter, LRC-OCN) with a pre-released version of CCSM4, which has the same ocean and sea-ice model resolution (1°) as LRC and the exact atmospheric and land model resolution (0.5°) as HRC (see details in Kirtman et al., 2012). LRC-OCN has a present-day control simulation of 150 years, and the first 50-years are taken as spin-up periods.

3 Results and Discussion

We first show the observed (GPCC and GPCP) and model simulated (HRC and LRC) decadal variance of rainfall over the SEUS and western North Atlantic in Figure 1 (left panels). We removed any linear trend from the datasets and applied a 5-year low-pass Butterworth filter to the anomalies to represent internal rainfall variability at decadal timescales. Here we define the SEUS as land regions bounded by 25°N to 38°N and 266°E to 284°E. Compared with both observational estimates, the model simulations generally show smaller decadal variance. CMIP5 multi-model mean estimates (based on thirty model historical simulations in Table S1) show 21% lower decadal SEUS rainfall variance than observational estimates based on GPCP. Overall, CMIP5 models (73%), including CCSM4, underestimate decadal rainfall variance in the SEUS.

We identify an increase in the decadal variance of the SEUS rainfall in HRC compared to LRC (Figs. 1c and 1d). Whether this improvement is due to finer ocean resolution remains unassessed in Fig. 1 given that both the atmospheric and oceanic resolutions are different between LRC and HRC. However, the role of the ocean resolution is isolated in Fig. S1a. Here we note that the slightly larger decadal variance in SEUS rainfall detected in LRC-OCN (0.5° atmosphere; Fig. S1) compared to LRC (1° atmosphere; Fig. 1d) implies that the increased atmospheric resolution is also partially responsible for the increased variance, but the resolved ocean meso-scale features also remain important. We also note that even though the decadal SEUS rainfall variability is slightly larger in LRC-OCN compared to LRC, the rainfall climatology only indicates small differences (not shown).

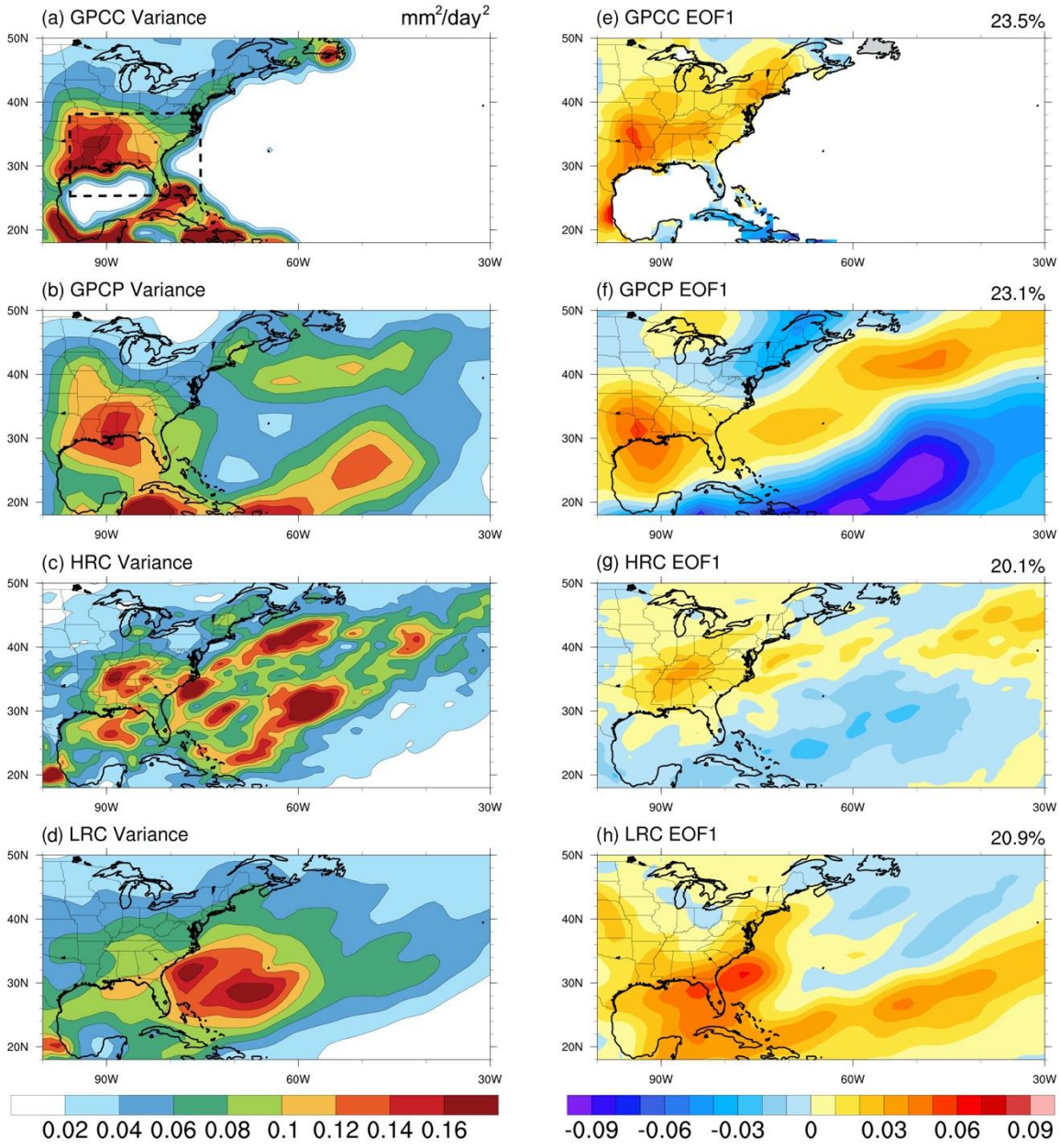

Figure 1. Decadal variance and leading EOF patterns (unit: mm/day) of monthly rainfall anomalies over the Southeast US and western North Atlantic region: (a, e) GPCP, (b, f) GPCP, (c, g) LRC, and (d, h) HRC. The land region within the black dashed box (25°N to 38°N, 266°E to 284°E) indicates the region of the Southeast US.

The leading spatial pattern of decadal rainfall variability (EOF1) in HRC (Fig. 1g) suggests that a tilted zonal dipole over the ocean in HRC, similar to the GPCP observations (Fig. 1f), is possibly linked to the Gulf Stream with maximum rainfall over the SEUS. However, the signal is weaker over SEUS than observational estimates (Figs. 1e and 1f). The center of action in LRC (and LRC-OCN, Fig. S1b) is further

south and east of the observed and HRC, and indicates relatively weak connectivity with the Gulf Stream. Based on these differences we hypothesize that resolved mesoscale processes in the Gulf Stream affect the center of decadal rainfall variability upstream and over SEUS.

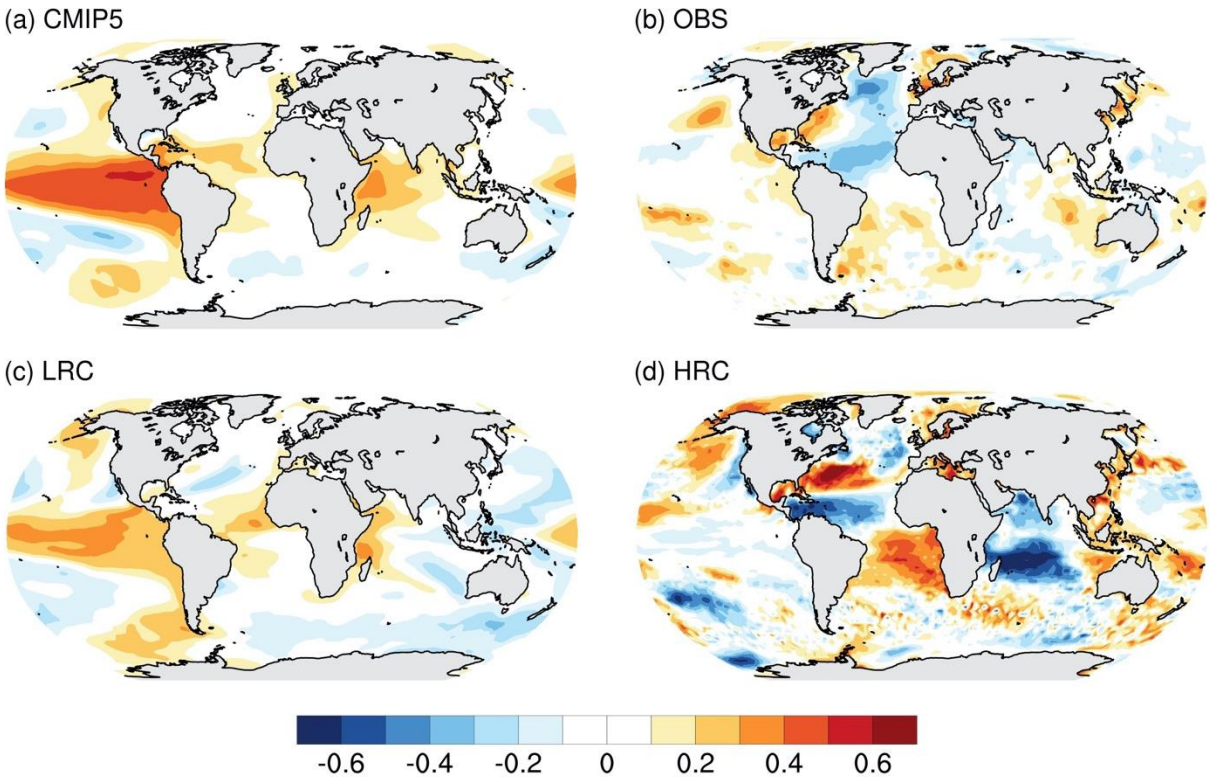

Figure 2. Correlation between decadal Southeast US rainfall index (25°-38°N, 266°-284°E) and global SST anomalies based on (a) CMIP5 (median correlation coefficients at each grid for thirty CMIP5 models), (b) OBS, (c) LRC, and (d) HRC. All the data have been applied with a 5-year low-pass filter. The maps only show the 95% confidence interval for the correlations based on the Student's *t* test (two-tailed).

To examine the role of SST variability in modulating decadal SEUS rainfall, we show in Figure 2 the correlation between decadal SEUS rainfall index and global SST anomalies for the observational estimates and the models, with shading significant at 95% confidence level based on the Student's *t* test (two-tailed). The decadal SEUS rainfall index is defined as the area-averaged values of 5-year low-pass filtered rainfall anomalies over the SEUS (25°-38°N, 266°-284°E) land points. Both LRC and CMIP5 models (median correlation coefficients for thirty CMIP5 models) show a strong correlation between the decadal SEUS rainfall index and the (ENSO-like) eastern tropical Pacific SST anomalies (Figs. 2a and 2c). A similar pattern is also identified with LRC-OCN with finer atmospheric resolution than LRC (not shown). This dominant role of ENSO SST in decadal SEUS rainfall in LRC and CMIP5 models can be attributed to

the typical strong wintertime connection between ENSO and SEUS rainfall that may persist on decadal timescales (Fig. S2). During boreal winter, near the peak of El Niño events, warm tropical SSTs affect the corresponding tropical convection, leading to a shift in the subtropical jet streams that brings more moisture to the SEUS (e.g., Infanti & Kirtman, 2019; Ropelewski & Halpert, 1986; Schmidt et al., 2001). La Niña generally leads to the opposite response.

However, the strong positive link between the decadal SEUS rainfall index and ENSO SST signal is weak or even missing in HRC and observational estimates (Figs. 2b and 2d). Interestingly, HRC and observational estimates suggests that decadal SST in the Gulf Stream and its surrounding regions can be the dominant contributor to decadal SEUS rainfall variability. We note that the correlation between decadal SEUS rainfall and Gulf Stream SST is detected in HRC is stronger than observational estimates, possibly because the spatial resolution of the currently available observed SST dataset – HadISST – is still too low to reproduce realistic decadal SST variability (Deser et al., 2010; Solomon & Newman, 2012), but we cannot eliminate the possibility that HRC overemphasizes the importance of the Gulf Stream variability. Nevertheless, HRC produces an improvement of decadal SEUS rainfall induced teleconnections compared with LRC, indicating the significant impact of ocean mesoscales on the SEUS rainfall-SST teleconnections. We further argue that LRC and most CMIP5 models may overestimate the role of tropical Pacific SST in the SEUS rainfall over decadal timescales. This overestimation can be explained by the classical wintertime connection between SEUS rainfall and tropical Pacific SST anomalies due to ENSO (Fig. S2). A similar finding was presented by Infanti and Kirtman (2019), who argued that instead of tropical Pacific SST, the Gulf Stream played a leading role in the 36-month prediction of the SEUS drought based on high-resolution CCSM4 initialized prediction experiments.

The influence of the NASH on interannual variations of the SEUS rainfall has been discussed in several earlier studies (e.g., Li et al., 2011; Li et al., 2012). Here we aim to investigate the role of the NASH in decadal SEUS rainfall variability by comparing HRC with LRC. We focus on 850 mb geopotential heights as it is a common indicator for the NASH. Figure 3 shows the composite of standardized decadal 850hPa geopotential height anomalies during wet and dry conditions over the SEUS. The corresponding composite of standardized decadal SST anomalies during wet and dry conditions is also shown in Figure S3. During the SEUS wet conditions, the warm SST and strong high-pressure anomalies along the Gulf of Mexico, SEUS, and Gulf Stream in HRC produce increased northward moisture transport and low-level convergence, which leads to upward motion and ultimately more precipitation over the SEUS. We argue this increased rainfall is due to the westward extension of the NASH (Li et al., 2011; Li et al., 2012; Jones, 2019). During the SEUS dry conditions, we find cold SST anomalies along the Gulf Stream and a robust low-pressure anomaly centered around the Gulf Stream extension in HRC, contributing to southward flow (with dry moisture advection) and low-level divergence and thus downward motion and less precipitation over the SEUS. HRC generally resembles the spatial patterns of the NASH variability based on observational estimates (Figs. 3a-d), though HRC somewhat overestimates the amplitude of the decadal NASH pressure anomalies and its connection to the SEUS rainfall (Figs. 4a and 4b).

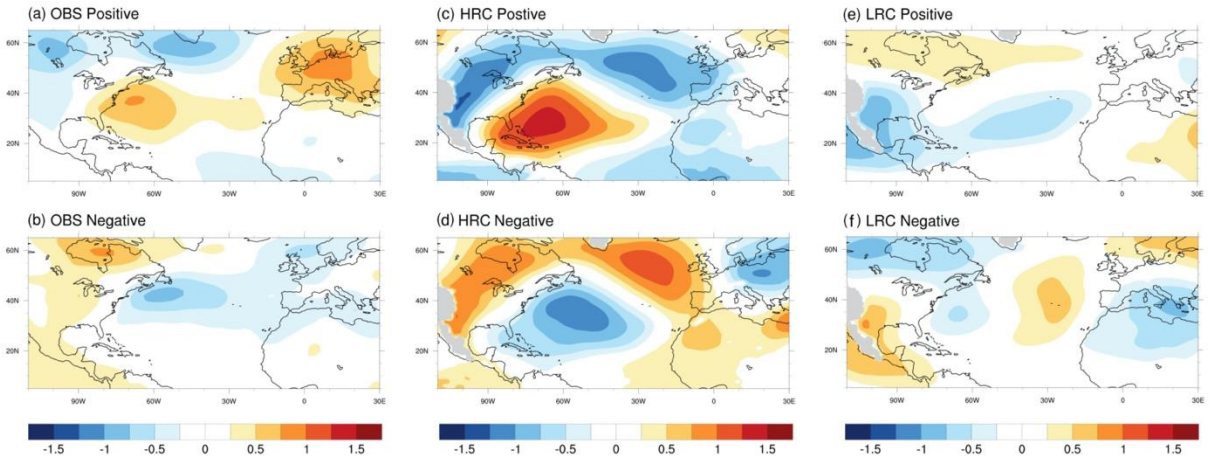

Figure 3. Composite of standardized decadal 850hPa geopotential height anomalies (unit: m) during wet and dry conditions over the SEUS based on (a, b) OBS, (c, d) HRC, and (e, f) LRC. Wet (dry) condition is identified when decadal SEUS rainfall index is above (below) plus (minus) one standard deviation.

LRC, conversely, fails to capture decadal NASH variability and its connection to the SEUS rainfall. For example, as seen in Figure 4, LRC largely fails to capture the westward expansion or shift of the NASH that is apparent in the observational estimates and in HRC. Changes in decadal SEUS rainfall in LRC are possibly due to variations of the pressure anomaly centers over the western US (Figs. 3e and 3f) and tropics.

Comparison between LRC and HRC suggests that a resolved Gulf Stream may improve the representation of the NASH that affects decadal SEUS rainfall. The resolved Gulf Stream in HRC influences the boundary layer, driving a nearly barotropic circulation response, and bringing more moisture, and ultimately increasing the SEUS rainfall owing to the westward extension of the NASH, as shown conceptually in Figure 5. It is possible that the North Atlantic Oscillation (NAO) can play a role in decadal SEUS rainfall variability (e.g., Hurrell & Van, 1997; Ning & Bradley, 2016; Whan & Zwiers, 2017), though we find no significantly larger NAO amplitude in HRC compared with LRC.

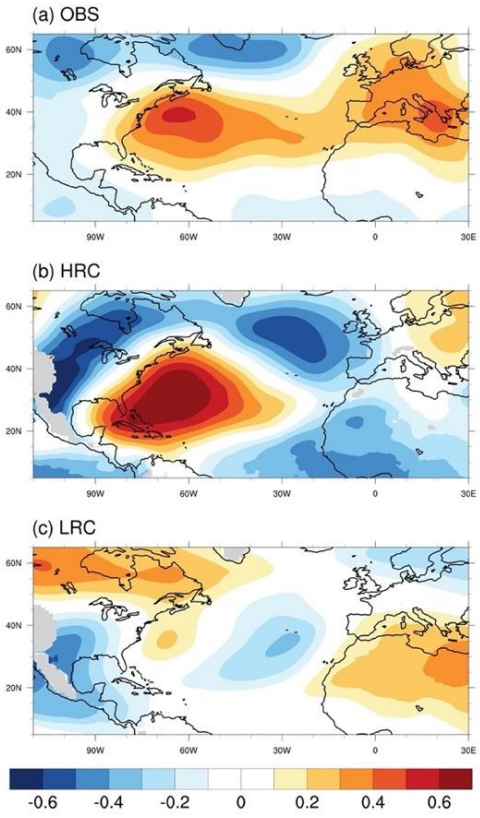

Figure 4. Correlation between decadal Southeast US rainfall index and 850hPa geopotential height anomalies based on (a) OBS, (b) HRC, and (c) LRC. The maps only show the correlation at the 95% level based on the Student's *t* test (two-tailed).

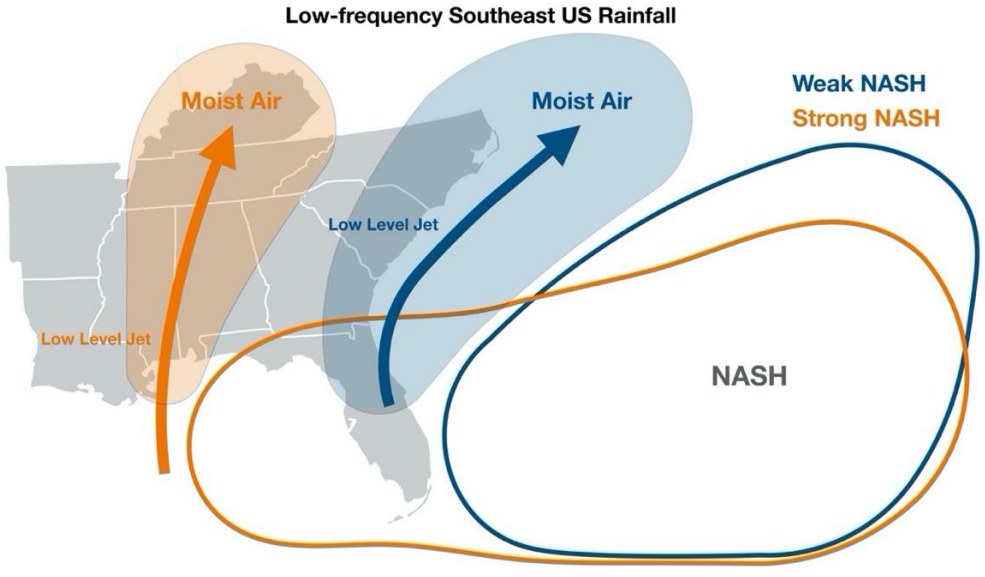

Figure 5. Diagram of the westward extension of the NASH for increased rainfall over the Southeast US.

4 Summary and Conclusion

This study investigates decadal SEUS rainfall and its teleconnections using high-resolution eddying CCSM4 simulations compared with its lower-resolution counterparts that are eddy parameterized. The inclusion of ocean mesoscales produces more realistic and warmer SST, sharper SST gradient (Siqueira & Kirtman, 2016), improved surface wind speed-SST coupling (Bryan et al., 2010), and better-represented subsurface ocean thermal and vertical structures (Zhang et al., 2021) along the Gulf Stream and its extension. An increase in decadal SST variance is also detected with HRC compared to LRC (not shown), especially along the Gulf Stream extension region.

With a better resolved Gulf Stream, the simulations indicate an improved annual mean rainfall climatology that is generally consistent with observational estimates. We find no notable improvement in the annual mean rainfall climatology over the SEUS, whereas enhanced decadal SEUS rainfall variance is detected with HRC in better agreement with observational estimates. Though atmospheric resolution may partly contribute to the increase in the decadal variance of the SEUS rainfall, the leading EOF pattern in HRC shows consistency with observations, indicating the influence of the resolved Gulf Stream with a local maximum over the SEUS. This dominant rainfall pattern in HRC and observational estimates is not the leading pattern in LRC or LRC-OCN, and thus, we conclude that this decadal variability is connected to resolved Gulf Stream variability.

The above conclusion is further supported by the decadal SEUS rainfall teleconnections with global SST. Consistent with Infanti and Kirtman (2019), the SEUS rainfall shows a higher correlation with the North Atlantic SST than the tropical Pacific SST on decadal timescales in HRC and observations. HRC suggests an even higher correlation between decadal SEUS rainfall and the Gulf Stream SST than observational estimates, perhaps indicating that HRC over-predicts the connectivity between Gulf Stream variability and decadal SEUS rainfall variability. Conversely, LRC and CMIP5 models overestimate the role of tropical Pacific SST in decadal SEUS rainfall due to the classic wintertime connection between the SEUS rainfall and ENSO. Although the seasonality of decadal SEUS rainfall is not our focus in this manuscript, we re-examine the SEUS rainfall-SST relationship in the summer and winter seasons, respectively (Fig. S2). Perhaps surprising is that the overall correlation patterns, as shown in Figure 2, pick up the wintertime relationships (Fig. S2). Interestingly, HRC and observation show a positive (negative) correlation between the SEUS rainfall and tropical Pacific SST during winter (summer), which may explain why decadal SEUS rainfall shows no discernable connection with ENSO SST.

A resolved Gulf Stream has both a localized impact and a remote circulation response affecting the SEUS. The resolved Gulf Stream influences the boundary layer and forces a near barotropic circulation response, and ultimately modulates the SEUS rainfall over decadal timescales. The representation of the NASH and its connection to the SEUS rainfall are improved in HRC with better represented ocean mesoscales. HRC can generally reproduce the observed westward extension and retreat of the NASH that regulates the variations of decadal SEUS rainfall (Figs. 3-5), despite that HRC may overestimate the correlation

between the SEUS rainfall and NASH. As suggested in HRC and observations, the westward extension of the NASH brings increased northward moisture transport and low-level convergence, leading to rising motion and ultimately more rainfall in the SEUS, which can be explained by a steady-state quasi-geostrophic balance. However, the LRC simulation fails to capture the realistic Gulf Stream, the westward extension of the NASH, and its relationship with the SEUS rainfall.

Uncertainty remains in this study as the length of high-resolution observation and model simulations is limited, and the results may be model-dependent. Many other factors that may influence decadal SEUS rainfall such as tropical cyclone activities and surface soil moisture are not addressed. However, this study, for the first time, demonstrates the potential benefits of an ocean eddying GCMs for regional rainfall simulations and predictions over land. Arguably, the results presented here demonstrate that using models that capture oceanic mesoscale features have the potential to improve the representation of rainfall variability remotely and regionally. How well this translates across models remains an open question and whether this improved simulated low-frequency variability of remote rainfall translates into improved predictions remains an open question.

Acknowledgements

This report is prepared by Wei Zhang under award NA18OAR4320123 from the National Oceanic and

Atmospheric Administration, U.S. Department of Commerce. The statements, findings, conclusions, and recommendations are those of the author(s) and do not necessarily reflect the views of the National Oceanic and Atmospheric Administration, or the U.S. Department of Commerce. Ben Kirtman and Leo Siqueira acknowledge the support from NOAA (NA18OAR4310293, NA15OAR4320064), NSF (OCE1419569, OCE1559151), and DOE (DE-SC0019433). We thank Nathaniel C. Johnson and Yongqiang Sun from NOAA GFDL for providing internal review.

All the observational, reanalysis data and CMIP5 historical simulations are properly referenced and publicly available. The GPCP and GPCC precipitation datasets are downloaded through https://psl.noaa.gov/data/gridded/data.gpcp.html and https://psl.noaa.gov/data/gridded/data.gpcc.html, respectively. The twentieth century reanalysis of geopotential height at 850 hPa can be found from NOAA's Physical Sciences Laboratory (https://psl.noaa.gov/data/20thC_Rean). Thirty CMIP5 model historical simulations and the associated model descriptions can be obtained from the Natural Environment Research Council's Data Repository for Atmospheric Science and Earth Observation (http://archive.ceda.ac.uk). The southeast US rainfall index (5-year low-pass filtered) derived from observations and models can be accessed by using the DOI http://doi.org/10.5281/zenodo.4433147. Besides, the model codes of CCSM4 used in this study can be achieved freely from http://www.cesm.ucar.edu/models/ccsm4.0/. The CCSM4 HRC and LRC model codes, experiments, and data outputs are archived at the University of Miami Center for Computational Science, which are available from the authors upon request.

References

Adler, R. F., Sapiano, M. R., Huffman, G. J., Wang, J. J., Gu, G., Bolvin, D., ... & Xie, P. (2018). The Global Precipitation Climatology Project (GPCP) monthly analysis (new version 2.3) and a review of 2017 global precipitation. Atmosphere, 9(4), 138. https://doi.org/10.3390/atmos9040138

Battisti, D. S., Vimont, D. J., & Kirtman, B. P. (2019). 100 Years of progress in understanding the dynamics of coupled atmosphere–ocean variability. Meteorological Monographs, 59, 8-1. https://doi.org/10.1175/AMSMONOGRAPHS-D-18-0025.1

Bryan, F. O., Tomas, R., Dennis, J. M., Chelton, D. B., Loeb, N. G., & McClean, J. L. (2010). Frontal scale air–sea interaction in high-resolution coupled climate models. Journal of Climate, 23(23), 6277-6291. https://doi.org/10.1175/2010JCLI3665.1

Burgman, R. J., & Jang, Y. (2015). Simulated US drought response to interannual and decadal Pacific SST variability. Journal of Climate, 28(12), 4688-4705. https://doi.org/10.1175/JCLI-D-14-00247.1

Chan, S. C., & Misra, V. (2010). A diagnosis of the 1979–2005 extreme rainfall events in the southeastern United States with isentropic moisture tracing. Monthly Weather Review, 138(4), 1172-1185.

https://doi.org/10.1175/2009MWR3083.1

Compo, G. P., Whitaker, J. S., Sardeshmukh, P. D., Matsui, N., Allan, R. J., Yin, X., ... & Brönnimann, S. (2011). The twentieth century reanalysis project. Quarterly Journal of the Royal Meteorological Society, 137(654), 1-28. https://doi.org/10.1002/qj.776

Delworth, T. L., Rosati, A., Anderson, W., Adcroft, A. J., Balaji, V., Benson, R., ... & Vecchi, G. A. (2012). Simulated climate and climate change in the GFDL CM2. 5 high-resolution coupled climate model. Journal of Climate, 25(8), 2755-2781. https://doi.org/10.1175/JCLI-D-11-00316.1

Deser, C., Phillips, A. S., & Alexander, M. A. (2010). Twentieth century tropical sea surface temperature trends revisited. Geophysical Research Letters, 37(10). https://doi.org/10.1029/2010GL043321

Feliks, Y., Ghil, M., & Robertson, A. W. (2011). The atmospheric circulation over the North Atlantic as induced by the SST field. Journal of Climate, 24(2), 522-542. https://doi.org/10.1175/2010JCLI3859.1

Fuentes-Franco, R., Giorgi, F., Coppola, E., & Kucharski, F. (2016). The role of ENSO and PDO in variability of winter precipitation over North America from twenty first century CMIP5 projections. Climate Dynamics, 46(9-10), 3259-3277. https://doi.org/10.1007/s00382-015-2767-y

Grondona, M. O., Podestá, G. P., Bidegain, M., Marino, M., & Hordij, H. (2000). A stochastic precipitation generator conditioned on ENSO phase: a case study in southeastern South America. Journal of Climate, 13(16), 2973-2986. https://doi.org/10.1175/1520-0442(2000)013<2973:ASPGCO>2.0.CO;2

Hawkins, E., & Sutton, R. (2011). The potential to narrow uncertainty in projections of regional precipitation change. Climate Dynamics, 37(1-2), 407-418. https://doi.org/10.1007/s00382-010-0810-6

He, J., Kirtman, B., Soden, B. J., Vecchi, G. A., Zhang, H., & Winton, M. (2018). Impact of ocean eddy resolution on the sensitivity of precipitation to CO2 increase. Geophysical Research Letters, 45(14), 7194-7203. https://doi.org/10.1029/2018GL078235

Hoerling, M. P., Kumar, A., & Zhong, M. (1997). El Niño, La Niña, and the nonlinearity of their teleconnections. Journal of Climate, 10(8), 1769-1786. https://doi.org/10.1175/1520-0442(1997)010<1769:ENOLNA>2.0.CO;2

Hurrell, J. W., & Van Loon, H. (1997). Decadal variations in climate associated with the North Atlantic Oscillation. In Climatic change at high elevation sites (pp. 69-94). Springer, Dordrecht.

Infanti, J. M., & Kirtman, B. P. (2016). North American rainfall and temperature prediction response to the diversity of ENSO. Climate Dynamics, 46(9-10), 3007-3023. https://doi.org/10.1007/s00382-015-2749-0

Infanti, J. M., & Kirtman, B. P. (2019). A comparison of CCSM4 high-resolution and low-resolution predictions for south Florida and southeast United States drought. Climate Dynamics, 52(11), 6877-6892. https://doi.org/10.1007/s00382-018-4553-0

Johnson, N. C., Krishnamurthy, L., Wittenberg, A. T., Xiang, B., Vecchi, G. A., Kapnick, S. B., & Pascale, S. (2020). The impact of sea surface temperature biases on North American precipitation in a high-resolution climate model. Journal of Climate, 33(6), 2427-2447. https://doi.org/10.1175/JCLI-D-19-0417.1

Jones, C. (2019). Recent changes in the South America low-level jet. npj Climate and Atmospheric Science, 2(1), 1-8. https://doi.org/10.1038/s41612-019-0077-5

Kirtman, B. P., Bitz, C., Bryan, F., Collins, W., Dennis, J., Hearn, N., ... & Stan, C. (2012). Impact of ocean model resolution on CCSM climate simulations. Climate Dynamics, 39(6), 1303-1328. https://doi.org/10.1007/s00382-012-1500-3

Kirtman, B. P., Perlin, N., & Siqueira, L. (2017). Ocean eddies and climate predictability. Chaos: An Interdisciplinary Journal of Nonlinear Science, 27(12), 126902. https://doi.org/10.1063/1.4990034

Knight, D. B., & Davis, R. E. (2007). Climatology of tropical cyclone rainfall in the southeastern United States. Physical Geography, 28(2), 126-147. https://doi.org/10.2747/0272-3646.28.2.126

Knutti, R., & Sedláček, J. (2013). Robustness and uncertainties in the new CMIP5 climate model projections. Nature Climate Change, 3(4), 369-373. https://doi.org/10.1038/nclimate1716

Koster, R. D., Dirmeyer, P. A., Guo, Z., Bonan, G., Chan, E., Cox, P., ... & Liu, P. (2004). Regions of strong coupling between soil moisture and precipitation. Science, 305(5687), 1138-1140. https://doi.org/10.1126/science.1100217

Kushnir, Y., Scaife, A. A., Arritt, R., Balsamo, G., Boer, G., Doblas-Reyes, F., ... & Matei, D. (2019). Towards operational predictions of the near-term climate. Nature Climate Change, 9(2), 94-101. https://doi.org/10.1038/s41558-018-0359-7

Kwon, H. H., Lall, U., & Obeysekera, J. (2009). Simulation of daily rainfall scenarios with interannual and multidecadal climate cycles for South Florida. Stochastic Environmental Research and Risk Assessment, 23(7), 879-896. https ://doi.org/10.1007/s0047 7-008-0270-2.

Li, L., Li, W., & Kushnir, Y. (2012). Variation of the North Atlantic subtropical high western ridge and its implication to Southeastern US summer precipitation. Climate Dynamics, 39(6), 1401-1412. https://doi.org/10.1007/s00382-011-1214-y

Li, W., Li, L., Fu, R., Deng, Y., & Wang, H. (2011). Changes to the North Atlantic subtropical high and its role in the intensification of summer rainfall variability in the southeastern United States. Journal of Climate, 24(5), 1499-1506. https://doi.org/10.1175/2010JCLI3829.1

Mamalakis, A., Yu, J. Y., Randerson, J. T., AghaKouchak, A., & Foufoula-Georgiou, E. (2018). A new interhemispheric teleconnection increases predictability of winter precipitation in southwestern US. Nature Communications, 9(1), 1-10. https://doi.org/10.1038/s41467-018-04722-7

Minobe, S., Kuwano-Yoshida, A., Komori, N., Xie, S. P., & Small, R. J. (2008). Influence of the Gulf Stream on the troposphere. Nature, 452(7184), 206-209. https://doi.org/10.1038/nature06690

Ning, L., & Bradley, R. S. (2016). NAO and PNA influences on winter temperature and precipitation over the eastern United States in CMIP5 GCMs. Climate dynamics, 46(3-4), 1257-1276. https://doi.org/10.1007/s00382-015-2643-9

Nogueira, R. C., & Keim, B. D. (2011). Contributions of Atlantic tropical cyclones to monthly and seasonal

rainfall in the eastern United States 1960–2007. Theoretical and Applied Climatology, 103(1-2), 213-227. https://doi.org/10.1007/s00704-010-0292-9

Pathak, R., Sahany, S., Mishra, S. K., & Dash, S. K. (2019). Precipitation Biases in CMIP5 Models over the South Asian Region. Scientific Reports, 9(1), 1-13. https://doi.org/10.1038/s41598-019-45907-4

Roberts, M. J., Jackson, L. C., Roberts, C. D., Meccia, V., Docquier, D., Koenigk, T., ... & Drijfhout, S. (2020). Sensitivity of the Atlantic meridional overturning circulation to model resolution in CMIP6 HighResMIP simulations and implications for future changes. Journal of Advances in Modeling Earth Systems, 12(8), e2019MS002014. https://doi.org/10.1029/2019MS002014

Ropelewski, C. F., & Halpert, M. S. (1986). North American precipitation and temperature patterns associated with the El Niño/Southern Oscillation (ENSO). Monthly Weather Review, 114(12), 2352-2362. https://doi.org/10.1175/1520-0493(1986)114<2352:NAPATP>2.0.CO;2

Scaife, A. A., & Smith, D. (2018). A signal-to-noise paradox in climate science. npj Climate and Atmospheric Science, 1(1), 28. https://doi.org/10.1038/s41612-018-0038-4

Scaife, A. A., Arribas, A., Blockley, E., Brookshaw, A., Clark, R. T., Dunstone, N., ... & Hermanson, L. (2014). Skillful long- range prediction of European and North American winters. Geophysical Research Letters, 41(7), 2514-2519. https://doi.org/10.1002/2014GL059637

Schmidt, N., Lipp, E. K., Rose, J. B., & Luther, M. E. (2001). ENSO influences on seasonal rainfall and river discharge in Florida. Journal of Climate, 14(4), 615-628. https://doi.org/10.1175/1520-0442(2001)014<0615:EIOSRA>2.0.CO;2

Schneider, U., Finger, P., Meyer-Christoffer, A., Rustemeier, E., Ziese, M., & Becker, A. (2017). Evaluating the hydrological cycle over land using the newly-corrected precipitation climatology from the Global Precipitation Climatology Centre (GPCC). Atmosphere, 8(3), 52. https://doi.org/10.3390/atmos8030052

Shepherd, T. G. (2014). Atmospheric circulation as a source of uncertainty in climate change projections. Nature Geoscience, 7(10), 703-708. https://doi.org/10.1038/ngeo2253

Siegert, S., Stephenson, D. B., Sansom, P. G., Scaife, A. A., Eade, R., & Arribas, A. (2016). A Bayesian framework for verification and recalibration of ensemble forecasts: How uncertain is NAO predictability?. Journal of Climate, 29(3), 995-1012. https://doi.org/10.1175/JCLI-D-15-0196.1

Siqueira, L., & Kirtman, B. P. (2016). Atlantic near- term climate variability and the role of a resolved Gulf Stream. Geophysical Research Letters, 43(8), 3964-3972. https://doi.org/10.1002/2016GL068694.

Siqueira, L., Kirtman, B. P., & Laurindo, L. C. (2021). Forecasting Remote Atmospheric Responses to Decadal Kuroshio Stability Transitions, Journal of Climate, 34(1), 379-395. https://doi.org/10.1175/JCLI-D-20-0139.1.

Small, R. D., deSzoeke, S. P., Xie, S. P., O'neill, L., Seo, H., Song, Q., ... & Minobe, S. (2008). Air–sea interaction over ocean fronts and eddies. Dynamics of Atmospheres and Oceans, 45(3-4), 274-319. https://doi.org/10.1016/j.dynatmoce.2008.01.001

Smith, D. M., Eade, R., Scaife, A. A., Caron, L. P., Danabasoglu, G., DelSole, T. M., ... & Kharin, V. (2019).

Robust skill of decadal climate predictions. npj Climate and Atmospheric Science, 2(1), 1-10. https://doi.org/10.1038/s41612-019-0071-y

Smith, D. M., Scaife, A. A., Eade, R., Athanasiadis, P., Bellucci, A., Bethke, I., ... & Danabasoglu, G. (2020). North Atlantic climate far more predictable than models imply. Nature, 583(7818), 796-800. https://doi.org/10.1038/s41586-020-2525-0

Solomon, A., & Newman, M. (2012). Reconciling disparate twentieth-century Indo-Pacific ocean temperature trends in the instrumental record. Nature Climate Change, 2(9), 691-699. https://doi.org/10.1038/nclimate1591

Strommen, K., & Palmer, T. N. (2019). Signal and noise in regime systems: A hypothesis on the predictability of the North Atlantic Oscillation. Quarterly Journal of the Royal Meteorological Society, 145(718), 147-163. https://doi.org/10.1002/qj.3414

Trenberth, K. E., Branstator, G. W., Karoly, D., Kumar, A., Lau, N. C., & Ropelewski, C. (1998). Progress during TOGA in understanding and modeling global teleconnections associated with tropical sea surface temperatures. Journal of Geophysical Research: Oceans, 103(C7), 14291-14324. https://doi.org/10.1029/97JC01444

Wang, S., Jing, Z., Zhang, Q., Chang, P., Chen, Z., Liu, H., & Wu, L. (2019). Ocean Eddy Energetics in the Spectral Space as Revealed by High-Resolution General Circulation Models. Journal of Physical Oceanography, 49(11), 2815-2827. https://doi.org/10.1175/JPO-D-19-0034.1

Whan, K., & Zwiers, F. (2017). The impact of ENSO and the NAO on extreme winter precipitation in North America in observations and regional climate models. Climate Dynamics, 48(5-6), 1401-1411. https://doi.org/10.1007/s00382-016-3148-x

Yoon, J. H., & Leung, L. R. (2015). Assessing the relative influence of surface soil moisture and ENSO SST on precipitation predictability over the contiguous United States. Geophysical Research Letters, 42(12), 5005-5013. https://doi.org/10.1002/2015GL064139

Zhang, W. (2020). Understanding Decadal Climate Predictability in the Global Ocean (Doctoral dissertation). Retrieved from ProQuest Dissertations & Theses Global (Order No. 28091098). Coral Gables, FL: University of Miami.

Zhang, W., & Kirtman, B. (2019a). Estimates of Decadal Climate Predictability from an Interactive Ensemble Model. Geophysical Research Letters, 46(6), 3387-3397. https://doi.org/10.1029/2018GL081307

Zhang, W., & Kirtman, B. (2019b). Understanding the Signal- to- Noise Paradox with a Simple Markov Model. Geophysical Research Letters, 46(22), 13308-13317. https://doi.org/10.1029/2019GL085159

Zhang, W., Kirtman, B., Siqueira, L., Clement, A., Xia, J. (2021). Understanding the Signal-to-Noise Paradox in Decadal Climate Predictability from CMIP5 and an Eddying Global Coupled Model. Climate Dynamics. https://doi.org/10.1007/s00382-020-05621-8

504

505